NOTES AND CORRESPONDENCE

A Generalization of the SLEVE Vertical Coordinate

DANIEL LEUENBERGER

MeteoSwiss, Zürich, Switzerland

MARCEL KOLLER*

Institute for Atmospheric and Climate Science, ETH Zürich, Zürich, Switzerland

OLIVER FUHRER

MeteoSwiss, Zürich, Switzerland

CHRISTOPH SCHÄR

Institute for Atmospheric and Climate Science, ETH Zürich, Zürich, Switzerland

(Manuscript received 8 December 2009, in final form 30 March 2010)

ABSTRACT

Most atmospheric models use terrain-following coordinates, and it is well known that the associated deformation of the computational mesh leads to numerical inaccuracies. In a previous study, the authors proposed a new terrain-following coordinate formulation [the smooth level vertical (SLEVE) coordinate], which yields smooth vertical coordinate levels at mid and upper levels and thereby considerably reduces numerical errors in the simulation of flow past complex topography. In the current paper, a generalization of the SLEVE coordinate is presented by using a modified vertical decay of the topographic signature with height. The new formulation enables an almost uniform thickness of the lowermost computational layers, while preserving the fast transition to smooth levels in the mid and upper atmosphere. This allows for a more consistent and more stable coupling with planetary boundary layer schemes, while retaining the advantages over classic sigma coordinates at upper levels. The generalized SLEVE coordinate is implemented and successfully tested in real-case simulations using an operational nonhydrostatic atmospheric model.

1. Introduction

The simulation of atmospheric flows over complex terrain using atmospheric models can be affected by truncation errors due to small-scale variations in the height of the terrain-following model levels. In a previous study (Schär et al. 2002, hereafter S02), we have demonstrated that the truncation error due to deformations of the computational mesh has the same leading order as the well-known truncation error that occurs with a uniform grid. As the two contributions have the same leading order, the mesh deformation may actually dominate the total truncation error. In the same study we have proposed a smooth level vertical (SLEVE) coordinate that significantly reduces such errors. The new coordinate uses a scale-dependent vertical decay of the model topography in the calculation of the level height, resulting in much smoother model levels in the middle and upper troposphere, as compared to the classical Gal-Chen coordinate (Gal-Chen and Somerville 1975) or hybrid coordinate systems.

Since the publication of S02 the SLEVE coordinate has been introduced in several models and a pressure-based coordinate version has also been developed (Zängl 2003). The SLEVE formulation has the ability to improve simulations of flow past complex topography in

* Current affiliation: Andritz Hydro AG, Zurich, Switzerland.

Corresponding author address: Daniel Leuenberger, MeteoSwiss, Krähbühlstrasse 58, 8044 Zürich, Switzerland.
E-mail: daniel.leuenberger@meteoswiss.ch

DOI: 10.1175/2010MWR3307.1

terms of the primary variables (S02; Zängl 2003), but also in terms of precipitation (Zängl 2004) or potential vorticity (Hoinka and Zängl 2004).

A general drawback of terrain-following coordinates is that the thickness of the lowest model layers can be substantially reduced above high mountain peaks. This issue is particularly germane with the SLEVE coordinate, as it employs much stronger low-level vertical compression. A weak compression of the lowest layer and thus a near homogeneous layer thickness is desirable for the following reasons. First, the thickness of the model layer may limit the maximum allowable time step of the vertical advection scheme and thus of the model as a whole. This is especially the case for convection resolving models, which can exhibit large vertical velocities. Second, large low-level fluxes of heat or momentum into thin model layers can cause very large tendencies of the model variables, possibly leading to numerical instabilities. This concern applies in particular to high mountain tops, where the horizontal wind may be very strong and the associated turbulent fluxes very large. Third, assumptions of the planetary boundary layer schemes may be violated if the first prognostic model level lies too close to the surface or outside of the surface layer. In particular, parameterizations of turbulent fluxes of momentum and heat based on Monin–Obukhov scaling (e.g., Louis 1979) require the depth of the lowest model level to be significantly larger than the roughness length at every grid point, which is difficult to ensure with the original SLEVE coordinate. Therefore, a strong compression of the lowest model layer is undesirable, as it potentially leads to unphysical results and/or numerical instability. The implications of these difficulties will depend upon details of the numerical implementation, the employed parameterization package, and the case under consideration. In our experience, however, compression of model layers often prevents the use of thin levels in the boundary layer, where a high vertical resolution would actually be crucial.

Several methods have been developed that avoid terrain-following grid transformations. Notable examples include the shaved cell method (e.g., Adcroft et al. 1997; Steppeler et al. 2002; Zhang and Rančić 2007) and the immersed boundary method (e.g., Lundquist et al. 2010). These methods avoid the compression of model layers, but they potentially suffer from other difficulties. For example, the model levels close to the earth's surface are not of uniform thickness.

This paper proposes a generalization of the SLEVE formulation, comparable to that proposed by Zängl (2003) in his pressure-based implementation. It reduces the compression of the lowest levels to a large extent, while retaining the attractive properties of the SLEVE coordinate in the upper atmosphere. In the following section we set out the definition along with some important properties of the new coordinate transformation. Section 3 presents the application in a high-resolution, operational numerical weather prediction setup, and section 4 provides some concluding remarks.

2. Definition of the coordinate

a. Basic formulation

The classic, height-based Gal-Chen coordinate is defined by $z(x, y, Z) = Z + h(x, y)b(Z)$, where z is the height, x and y are the horizontal coordinates, and Z is a height-based vertical coordinate, which is generally chosen to be nonequidistant, with many thin layers near the lower boundary and thicker layers aloft. The $h(x, y)$ is the model orography and $b(Z) = 1 - Z/Z_T$ may be interpreted as a decay function, which determines the vertical decay of topographic features with height. Here Z_T is the height of the model top. In the Gal-Chen formulation this decay is linear, leading to noisy level heights above complex topography, even at mid and upper levels.

The height-based, terrain-following coordinate formulation proposed in S02 reads

$$z(x, y, Z) = Z + h_1(x, y)b_1(Z) + h_2(x, y)b_2(Z). \quad (1)$$

Here the decay of topography is done separately for the smooth large-scale contribution of the model topography $h_1(x, y)$, and its small-scale counterpart $h_2(x, y)$. The large-scale contribution $h_1(x, y)$ is obtained from $h(x, y)$ with a digital filter and $h = h_1 + h_2$. The approach uses two vertical decay functions $b_i(Z)$ for the two topographic contributions h_i.

The new formulation proposed in this paper retains (1) but uses generalized decay functions:

$$b_i(Z) = \frac{\sinh[(Z_T/s_i)^n - (Z/s_i)^n]}{\sinh[(Z_T/s_i)^n]}, \quad (2)$$

where $n \geq 1$ is a real number and s_i are the decay constants of the respective topographic contributions. The original SLEVE formulation is represented by $n = 1$. To illustrate the potential difficulties with thin near-surface model layers, it is helpful to consider the derivative of (1) with respect to the vertical coordinate Z:

$$\frac{\partial z}{\partial Z} = 1 + h_1(x, y)\frac{\partial b_1}{\partial Z} + h_2(x, y)\frac{\partial b_2}{\partial Z}. \quad (3)$$

The thickness of model level k can then be written as $\Delta z_k \approx \Delta Z_k(\partial z/\partial Z)_k$, where ΔZ_k is the distance between levels k and $k - 1$ in absence of topography. From (3) it

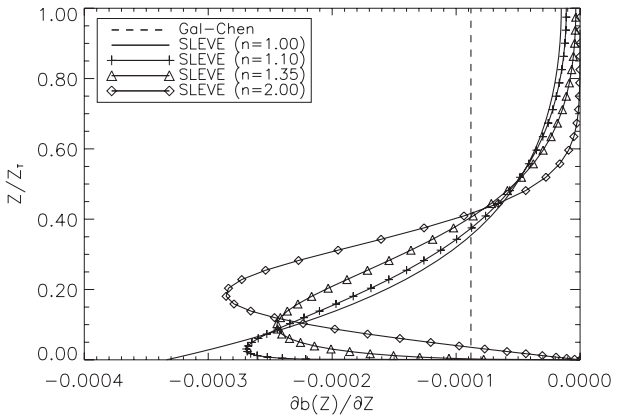

FIG. 1. Vertical derivatives of the decay functions $b(Z/Z_T)$ for the Gal-Chen (dashed line), SLEVE (solid line), and the generalized SLEVE coordinate with different values of n (crosses, triangles, and squares). For the SLEVE coordinates we use a vertical decay rate of $s/Z_T = 0.26$.

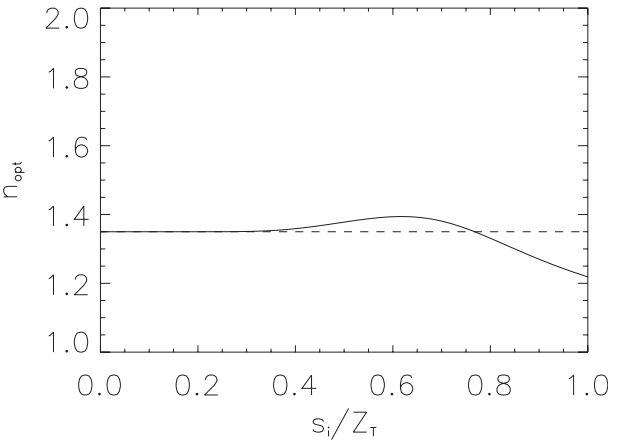

FIG. 2. Dependence of the optimal parameter n_{opt} upon the vertical decay rate s_i/Z_T.

is evident that the maximum compression of model layers with given topographic heights h_1 and h_2 is determined by the minima of

$$\frac{\partial b_i}{\partial Z} = \begin{cases} -\dfrac{n}{s_i^n} Z^{(n-1)} \dfrac{\cosh[(Z_T/s_i)^n - (Z/s_i)^n]}{\sinh[(Z_T/s_i)^n]} & \text{for} \quad n > 1 \\ -\dfrac{1}{s_i} \dfrac{\cosh(Z_T/s_i - Z/s_i)}{\sinh(Z_T/s_i)} & \text{for} \quad n = 1 \end{cases} . \tag{4}$$

Below we will analyze (4) for given topographic heights and decay rates. For this purpose it is sufficient to focus upon one of the two topographic contributions in (3), and we thus drop the subscript i.

Figure 1 illustrates $\partial b/\partial Z$ as a function of Z/Z_T for the Gal-Chen coordinate, the original SLEVE coordinate, and the generalized SLEVE coordinate with three different values of n. For the Gal-Chen coordinate, the compression is uniform throughout the atmosphere (dashed line in Fig. 1). For the original SLEVE formulation ($n = 1$) the minimum of (4) amounts to $-s^{-1}\coth(Z_T/s)$ and occurs at $Z = 0$, resulting in a strong compression of the lowest model layer. For $n > 1$ the term $\partial b/\partial Z$ vanishes at $Z = 0$, thereby drastically reducing the compression of the lowest model layer, while retaining some compression at higher levels. As the layer thickness usually increases with height (stretched vertical grid), the compression at higher levels is less critical. Figure 1 also shows that the height and strength of the maximum layer compression depend upon the choice of n. Thus, we may choose n such as to minimize the compression of the near-surface levels.

There are other criteria in optimizing the design of a vertical coordinate. For example, it is also desirable that model levels become horizontal at the lowest possible altitude. Moreover, the degree to which compression is considered undesirable depends on the amount of vertical coordinate stretching, so this could also be included in optimizing the vertical coordinate. Since strong compression of the lowest model level is the most severe drawback of the original SLEVE formulation, we concentrate here on the minimization of the level compression.

b. *Minimizing the compression of the near-surface levels*

We define an optimal value of n by requesting that the maximum layer compression occurring throughout the atmosphere is minimized. This implies that $n = n_{\text{opt}}$ is defined such as to maximize the expression $\min_Z[\partial b(Z, n; s)/\partial Z]$. For a given decay rate s, n_{opt} can be obtained by finding the saddle point of the two-dimensional function $\partial b_i(Z, n)/\partial Z$. Figure 2 shows the numerically derived n_{opt} as a function of s. Fortunately, n_{opt} only slightly depends upon s, at least within the typical range of parameters under consideration.

Thus we will set n in (2) to the value of $n_{\text{opt}} = 1.35$. The respective value has also been used in Fig. 1. In principle, it would be possible to optimize the coordinate by using two different values of n for the two terms in (1), but we doubt that this would significantly improve the formulation.

c. *Invertibility constraint*

Vertical coordinate transformations $z(Z)$ need to satisfy the invertibility condition $\partial z/\partial Z > 0$. For the SLEVE coordinate, the invertibility condition rules out too small values of the dimensionless decay parameters s_i/Z_T (see S02). Since the new formulation reduces the minima of $\partial b_i/\partial Z$, it also favorably influences the invertibility condition. Figure 3 shows contour plots of the invertibility parameter $\gamma = \min_z(\partial z/\partial Z)$ as a function of $(s_1/Z_T, s_2/Z_T)$, similar to Fig. 3 of S02. The plots are

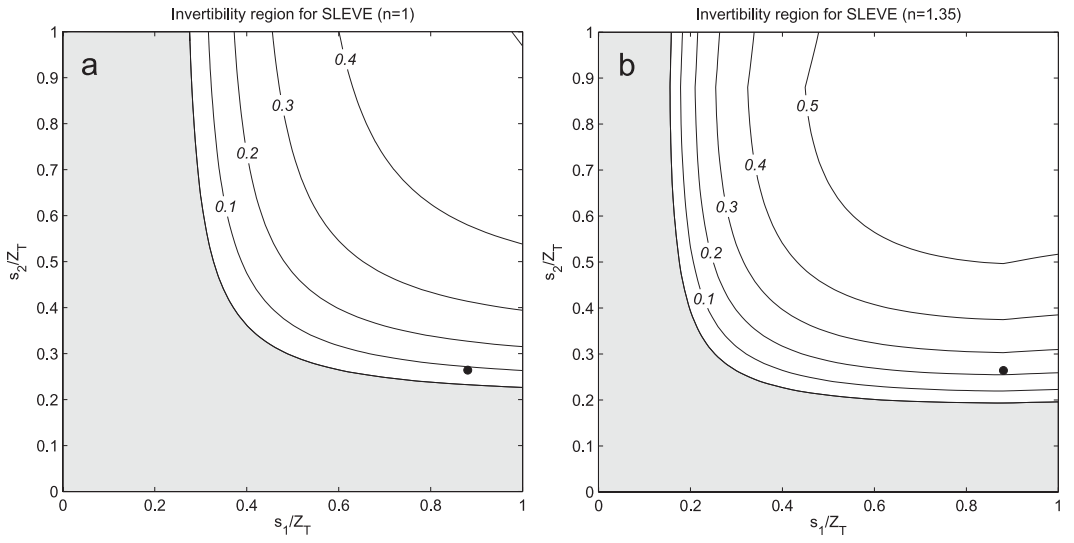

FIG. 3. Invertibility parameter γ for (a) the original ($n = 1$) and (b) the optimal ($n = 1.35$) SLEVE formulation. The gray fraction of parameter space is ruled out due to the lack of invertibility. The dimensionless values $h_{1,\max}/Z_T = 0.22$ and $h_{2,\max}/Z_T = 0.16$ result from the experiment described in section 3. The black dots in the regime diagrams correspond to $s_1 = 10\,000$ m and $s_2 = 3000$ m, resulting in an invertibility parameter of $\gamma = 0.08$ (0.22) for $n = 1$ (1.35).

for specific values of $h_{1,\max}/Z_T$ and $h_{2,\max}/Z_T$. Settings of (s_1/Z_T, s_2/Z_T) in the gray area violate the invertibility condition. Compared to the original formulation (Fig. 3a), the generalized SLEVE formulation (Fig. 3b) results in a larger admissible parameter range, and the higher values of γ demonstrate that the generalized SLEVE coordinate results in a less severe compression of the model levels. As a consequence the vertical decay parameters s_i can in principle be chosen smaller than with the original SLEVE formulation, leading to a faster transition to smoothness and eventually horizontal model levels with height.

3. Application in an NWP model

The generalized SLEVE coordinate has been tested in the nonhydrostatic NWP model of the Consortium for Small scale Modeling (COSMO; see online at http://www.cosmo-model.org; Doms and Schättler 2002; Steppeler et al. 2003) using the high-resolution operational setting at MeteoSwiss. The computational domain covers the Alpine region (Fig. 4) and is horizontally discretized using a computational mesh with a horizontal grid spacing of $\Delta x = 2.2$ km. The model top is located at roughly 23 km and 60 stretched vertical levels divide the atmosphere in layers, the lowest being 20 m thick.

The model version under consideration uses split-explicit dynamics with Runge–Kutta time stepping (Wicker and Skamarock 2002; Förstner and Doms 2004). Advection terms are discretized using a fifth-order upwind scheme in the horizontal and a implicit second-order centered scheme in the vertical. Smoothing using a monotonic fourth-order diffusion operator is applied within the first 26 grid points from the domain boundary. Inside the domain, no additional smoothing is applied. In terms of physical parameterizations, the model features the Ritter and Geleyn (1992) radiative transfer scheme, the TERRA-ML [the Biosphere–Atmosphere Transfer Scheme (BATS)] multilayer soil model (Schrodin and Heise 2002), vertical fluxes of momentum and heat based on turbulent kinetic energy (Raschendorfer 2001), and prognostic hydrometeors (Reinhardt and Seifert 2006).

COSMO employs a semi-implicit scheme for the vertical advection of the three wind components, pressure and temperature. For the advection of moisture variables and turbulent kinetic energy (TKE) it employs a semi-Lagrangian advection scheme. Both vertical advection schemes are unrestricted-time-step schemes (cf. Skamarock 2006) and, thus, stable for vertical Courant numbers exceeding unity. Other models employ a forward-in-time discretization of the vertical advection, and this implies that the time step may be severely constrained by very shallow vertical layers. In practice, these models typically limit the vertical advection velocity in order to ensure stability of the vertical advection scheme.

a. Geometry of model levels

Three vertical coordinate versions are compared: the traditional Gal-Chen coordinate, the SLEVE formulation ($n = 1$) of S02, and the generalized SLEVE formulation ($n = 1.35$). The coordinates are used in a hybrid setting (i.e., above $Z_T = 11\,357$ m) the model levels are horizontal until the model top at 23 588 m. For both SLEVE

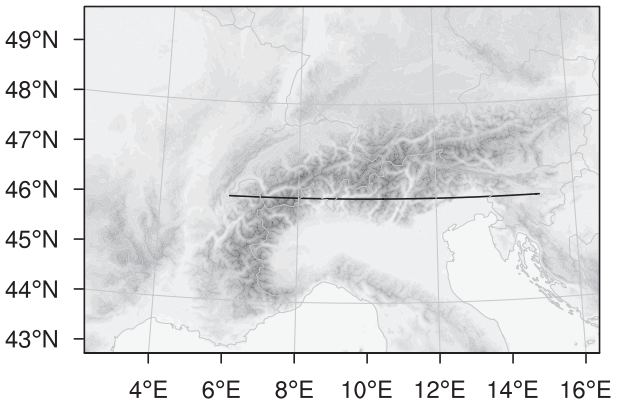

FIG. 4. Computational domain of the COSMO-2 experiments. Topography is shown in shaded contours and minimum and maximum height is displayed. The position of the vertical cross section used in Fig. 6 is marked with a bold solid line.

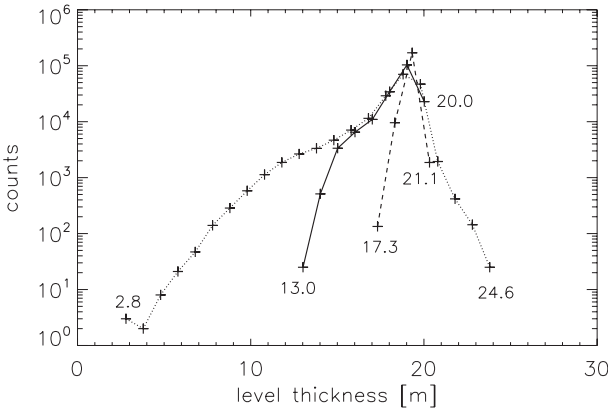

FIG. 5. Histograms for the thicknesses of the lowermost computational layer. The curves relate to the Gal-Chen (solid line), the original SLEVE ($n = 1$, dotted line), and the optimal SLEVE coordinate ($n = 1.35$, dashed line). The bin size of the histograms is 1 m. The maxima and minima of the respective thicknesses are displayed in the diagram.

versions we set $s_1 = 10\,000$ m and $s_2 = 3000$ m, resulting in invertibility parameters $\gamma = 0.08$ for $n = 1$ and $\gamma = 0.22$ for $n = 1.35$ (see black dots in Fig. 3). Following S02, the topography is split into a large-scale part h_1 with a maximum of 2462 m and a small-scale part h_2 with a maximum of 1836 m using multiple applications of a Laplace filter. Figure 5 shows a histogram of the frequency distribution of lowest model level thickness, along with its minima and maxima, representing all grid points of the computational domain. The generalized SLEVE formulation ($n = 1.35$, dashed line) yields a very narrow distribution [i.e., the thickness is much more uniform as compared to the Gal-Chen (solid line) and traditional SLEVE ($n = 1$, dotted line) coordinate]. The level thickness of $\Delta Z_1 = 20$ m is compressed to a minimum value of 13 m for the Gal-Chen coordinate, whereas in the SLEVE setting a minimum level thickness of 2.8 m is obtained. Using the optimal SLEVE formulation, the lowest model layer has a much more uniform depth with a minimum of 17.3 m.

Figures 6a–c show the vertical level distribution along a west–east cross section (black bold line in Fig. 4) for the three coordinate settings. In the Gal-Chen setting the finescale topographic variations are visible almost up to the model top, whereas both SLEVE formulations yield much smoother levels in the mid- and upper model domain. Note that as a consequence of the faster decay of $b_i(z)$ for $n > 1$, the new SLEVE formulation leads to even smoother upper levels.

b. Case study

Simulations with the three coordinate settings shown in Fig. 6 have been conducted for several cases. Even the SLEVE ($n = 1$) simulation with a minimum layer thickness of only 2.8 m could be stably integrated, probably due to the implicit vertical discretization in the COSMO model, and due to the fact, that only a few grid points exhibit such thin layers (see Fig. 5). Here we discuss in some detail a single case of strong northerly flow against the Alps.

The simulations were initialized on 0000 UTC 19 February 2009 from the interpolated, operational ECMWF analysis and integrated over a time period of 48 h. During the first 24 h, observations were continuously assimilated using the operational data assimilation scheme of COSMO-2. The simulations were driven at the lateral boundaries by a 7-km-resolution simulation, which in turn was driven by operational forecasts of ECMWF.

The right-hand panels of Fig. 6 show the resulting distributions of potential temperature at 0000 UTC 21 February 2009 in a vertical section running along the Alps (see Fig. 4). At first glance the three panels look rather similar (thus confirming the validity of our implementation). More detailed inspection reveals that the numerical solution with the Gal-Chen coordinate is considerably noisier (in particular at altitudes around 7 km), while the differences between the two SLEVE coordinate versions are insignificant.

For further analysis we consider kinetic energy spectra. Following Skamarock (2004), the spectra are computed using one-dimensional spectral decomposition of the velocities (u, v, w) interpolated onto constant z surfaces along the west–east and north–south grid lines spanning the domain. For each of the two directions, the energy densities are averaged vertically over 9 levels (from 6 to 10 km), horizontally over all grid lines, and temporally over the last 24 h of the integrations in 1-h intervals.

In Fig. 7 we show the resulting kinetic energy spectra in the north–south direction. Down to a wavelength of

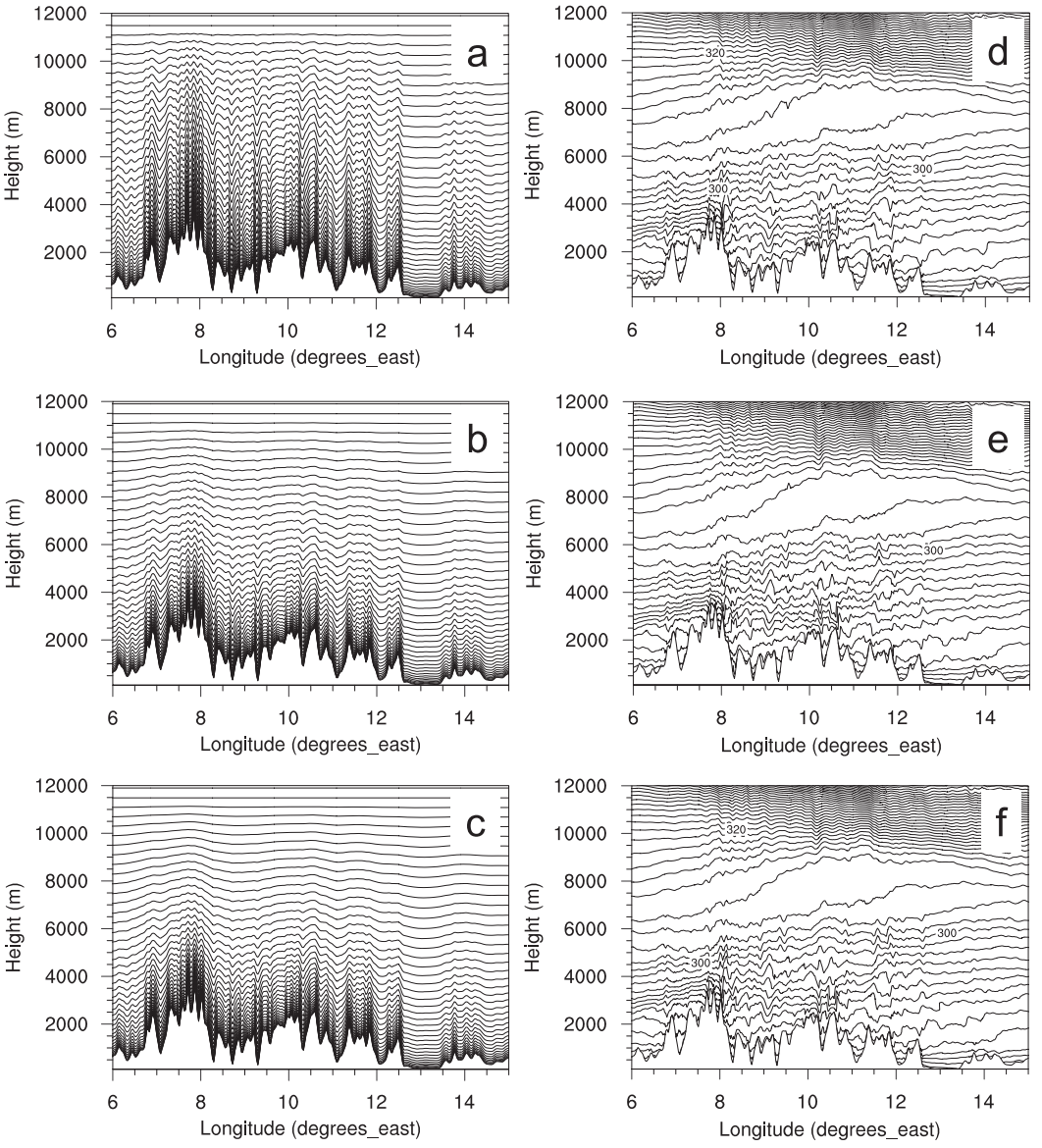

FIG. 6. Application of different vertical coordinate formulations in the COSMO-2 model over the Alps. (a),(d) The model grid using the Gal-Chen coordinate; (b),(e) the original SLEVE coordinate ($n = 1$); and (c),(f) the optimal SLEVE coordinate ($n = 1.35$). (a)–(c) Vertical levels in a cross section at 46.1°N (indicated in Fig. 4 by a bold line). (d)–(f) Distribution of potential temperature (in K) after 48-h integration in the same cross section. Note the smoother representation of the isentropic distribution in (e),(f) as compared to (d).

about $\lambda = k/2\pi = 7\Delta x$, the spectra roughly follow the $k^{-5/3}$ slope characteristic of the mesoscale, while at shorter scales it is determined by numerical dissipation (Skamarock 2004). In comparison to the SLEVE coordinates, the Gal-Chen coordinate (dotted line) shows a significantly higher energy density at the small-scale tail of the spectrum. The difference is largest near the shortwave cutoff at $2\Delta x$ (4.4 km), where it corresponds to more than half an order of magnitude. This demonstrates that the SLEVE coordinate considerably reduces small-scale noise that arises in response to numerical truncation errors due to the deformation of the computational grid.

4. Conclusions

In this paper, a generalized terrain-following SLEVE coordinate formulation for atmospheric models is proposed with a modified vertical decay of topographic variations with height, leading to a nearly uniform level thickness at low levels, while preserving the fast transition to smooth levels in the mid and upper atmosphere.

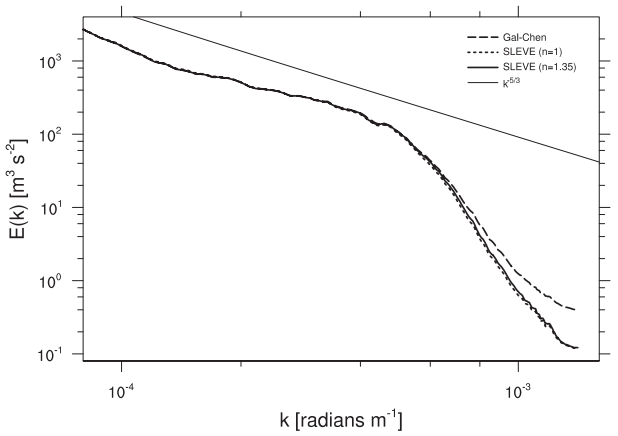

FIG. 7. Small-scale tail of the kinetic energy spectra in the north–south direction averaged vertically between 6 and 10 km, horizontally over the full domain, and temporally over the last 24-h period of the simulation. The three spectra shown depict the results of simulations that are identical except for using three different coordinate formulations (see legend). Note how the two SLEVE formulations achieve a significantly lower level of energy near the shortwave cutoff at $\lambda = 2\pi/k = 2\Delta x$ (4.4 km).

A near-uniform level thickness of the lowest levels is advantageous for various reasons.

In comparison to the original SLEVE coordinate, the generalized formulation dramatically reduces the compression of low-level model layers and thereby improves the numerical stability and the coupling to the boundary layer scheme. The optimized coordinate is particularly suited for stretched vertical coordinates, since the maximum compression is located some distance above the surface, where the model layers are usually thicker than near the surface. It is also suited for equidistant level distributions, since the maximum compression of the layers occurring in the vertical profile is reduced.

The optimized SLEVE formulation has been successfully tested in real-case simulations above complex topography using the convection-permitting, nonhydrostatic COSMO model, demonstrating the feasibility of the novel approach.

Acknowledgments. The simulations for this work have been conducted at the Swiss Center for Scientific Computing (CSCS, Manno, Switzerland). The comments of two anonymous reviewers have led to an improvement of the original manuscript and are kindly acknowledged.

REFERENCES

Adcroft, A., C. Hill, and J. Marshall, 1997: Representation of topography by shaved cells in a height coordinate ocean model. *Mon. Wea. Rev.,* **125,** 2293–2315.

Doms, G., and U. Schättler, 2002: A description of the nonhydrostatic regional model LM. Part I: Dynamics and numerics. COSMO, 134 pp. [Available online at http://www.cosmo-model.org/.]

Förstner, J., and G. Doms, 2004: Runge–Kutta time integration and high-order spatial discretization of advection—A new dynamical core for the LMK. *COSMO Newsletter,* No. 4, COSMO, 168–176. [Available online at http://www.cosmo-model.org/.]

Gal-Chen, T., and C.-J. Somerville, 1975: On the use of a coordinate transformation for the solution of the Navier–Stokes equations. *J. Comput. Phys.,* **17,** 209–228.

Hoinka, K.-P., and G. Zängl, 2004: The influence of the vertical coordinate on simulations of a PV streamer crossing the Alps. *Mon. Wea. Rev.,* **132,** 1860–1867.

Louis, J.-F., 1979: A parametric model of vertical eddy fluxes in the atmosphere. *Bound.-Layer Meteor.,* **17,** 187–202.

Lundquist, K. A., F. K. Chow, and J. K. Lundquist, 2010: An immersed boundary method for the Weather Research and Forecasting model. *Mon. Wea. Rev.,* **138,** 796–817.

Raschendorfer, M., 2001: The new turbulence parameterization of LM. *COSMO Newsletter,* No. 1, COSMO, 90–98. [Available online at http://www.cosmo-model.org/.]

Reinhardt, T., and A. Seifert, 2006: A three-category ice scheme for LMK. *COSMO Newsletter,* No. 6, COSMO, 115–120. [Available online at http://www.cosmo-model.org/.]

Ritter, B., and J. F. Geleyn, 1992: A comprehensive radiation scheme for numerical weather prediction models with potential applications in climate simulations. *Mon. Wea. Rev.,* **120,** 303–325.

Schär, C., D. Leuenberger, O. Fuhrer, D. Lüthi, and C. Girard, 2002: A new terrain-following vertical coordinate formulation for atmospheric prediction models. *Mon. Wea. Rev.,* **130,** 2459–2480.

Schrodin, R., and E. Heise, 2002: A new multi-layer soil-model. *COSMO Newsletter,* No. 2, COSMO, 149–151. [Available online at http://www.cosmo-model.org/.]

Skamarock, W. C., 2004: Evaluating mesoscale NWP models using kinetic energy spectra. *Mon. Wea. Rev.,* **132,** 3019–3032.

——, 2006: Positive-definite and monotonic limiters for unrestricted-time-step transport schemes. *Mon. Wea. Rev.,* **134,** 2241–2250.

Steppeler, J., H.-W. Bitzer, M. Minotte, and L. Bonaventura, 2002: Nonhydrostatic atmospheric modeling using a z-coordinate representation. *Mon. Wea. Rev.,* **130,** 2143–2149.

——, G. Doms, U. Schättler, H.-W. Bitzer, A. Gassmann, U. Damrath, and G. Gregoric, 2003: Meso-gamma scale forecasts using the nonhydrostatic model LM. *Meteor. Atmos. Phys.,* **82,** 75–96.

Wicker, L., and W. Skamarock, 2002: Time-splitting methods for elastic models using forward time schemes. *Mon. Wea. Rev.,* **130,** 2088–2097.

Zängl, G., 2003: A generalized sigma-coordinate system for the MM5. *Mon. Wea. Rev.,* **131,** 2875–2884.

——, 2004: The sensitivity of simulated orographic precipitation to model components other than cloud microphysics. *Quart. J. Roy. Meteor. Soc.,* **130,** 1857–1875.

Zhang, H., and M. Rančić, 2007: A global Eta model on quasi-uniform grids. *Quart. J. Roy. Meteor. Soc.,* **133,** 517–528.